Available online at www.sciencedirect.com
ScienceDirect
Acta Materialia 59 (2011) 6684–6690
Acta MATERIALIA
www.elsevier.com/locate/actamat

A phenomenological model of electronic band structure in ferroelectric $Pb(In_{1/2}Nb_{1/2})O_3$–$Pb(Mg_{1/3}Nb_{2/3})O_3$–$PbTiO_3$ single crystals around the morphotropic phase boundary determined by temperature-dependent transmittance spectra

J.J. Zhu [a], W.W. Li [a], G.S. Xu [b], K. Jiang [a], Z.G. Hu [a,*], J.H. Chu [a]

[a] Key Laboratory of Polar Materials and Devices, Ministry of Education, Department of Electronic Engineering, East China Normal University, Shanghai 200241, People's Republic of China
[b] R&D Center of Synthetic Crystals, Shanghai Institute of Ceramics, Chinese Academy of Sciences, Shanghai 201800, People's Republic of China

Received 17 June 2011; received in revised form 8 July 2011; accepted 12 July 2011
Available online 6 August 2011

Abstract

The optical properties of ferroelectric $Pb(In_{1/2}Nb_{1/2})O_3$–$Pb(Mg_{1/3}Nb_{2/3})O_3$–$PbTiO_3$ (PIN–PMN–PT) single crystals around the morphotropic phase boundary (MPB) have been investigated using ultraviolet–infrared transmittance spectra in the temperature range of 8–300 K. Based on the temperature-dependent spectral measurement of the band gap, we propose a phenomenological model of band structure vs. temperature to explain both the negative and positive band narrowing coefficient dE_{gd}/dT in ferroelectric PIN–PMN–PT crystals around the MPB where multiple phases coexist. The peculiar positive coefficient only exists in the fragile multiphase region of the MPB, while the negative coefficient, caused by thermal expansion of the lattice and renormalization of the band structure by electron–phonon interaction, exists in the rhombohedral or tetragonal single-phase region as well as in the stationary multiphase region of the MPB. The origin of the positive coefficient is a long-range increasing fraction of coexistence from the monoclinic phase with small band gap to rhombohedral phase with large band gap at elevated temperature. In agreement with optical transmittance results of PMN–PT/PIN–PMN–PT, the model predicts that these unusual positive band narrowing coefficients may exist for all ferroelectrics around the MPB where the coexistence of phases lacks thermodynamic stability.

Keywords: Ferroelectric; Phase coexistence; Optical spectroscopy; Electronic band structure; Temperature dependence

1. Introduction

Both negative and positive band gap narrowing trends are found in $Pb(In_{1/2}Nb_{1/2})O_3$–$Pb(Mg_{1/3}Nb_{2/3})O_3$–$PbTiO_3$ (PIN–PMN–PT) crystals around the morphotropic phase boundary (MPB). The positive band gap narrowing trend vs. temperature has attracted interest because most semiconductors show negative band gap narrowing trends. The negative band gap narrowing trend is usually explained by two factors: thermal expansion of the lattice, and renormalization of the band structure by electron–phonon interaction; the origin of the positive trend is more complicated [1]. $Pb_{1-x}Sn_xTe$ and $Hd_{1-x}Cd_xTe$ alloys are well-known narrow band gap semiconductors which have both negative and positive band gap narrowing trends depending on the SnTe/CdTe composition [2–4]. These alloys are a mixture of a semimetal (HgTe), which has a negative gap, with a semiconductor (CdTe), which has a positive one. The tin salt SnTe, which has a negative band narrowing trend, is usually compared with the lead salt PbTe as an example of the so-called band inversion. In PbTe, the symmetry of the top valence band is L_6^+ and that of the bottom

* Corresponding author. Tel.: +86 21 54345150; fax: +86 21 54345119.
E-mail address: zghu@ee.ecnu.edu.cn (Z.G. Hu).

1359-6454/$36.00
doi:10.1016/j.actamat.2011.07.025

conduction band is L_6^-; the ordering is reversed in SnTe. The band structures of HgTe and CdTe have a similar inversion. Obviously, the positive temperature shifts of ferroelectrics are not due to the band inversion which causes the positive temperature shifts in the narrow band gap semiconductors $Pb_{1-x}Sn_xTe$ and $Hd_{1-x}Cd_xTe$ alloys.

On the other hand, relaxor ferroelectric crystals of perovskite-type (Fig. 1) close to the MPB, which separates regions of tetragonal symmetry from those of rhombohedral symmetry by varying the composition, have been widely studied because of their superior piezoelectric properties [5,6]. The high piezoelectricity is related to the polarization rotation mechanism, in contrast to the electromechanical coupling through ionic displacements and the associated lattice distortion along the polar direction in conventional piezoelectric materials [7,8]. PIN–PMN–PT single crystal, the MPB of which is located between PIN–0.37PT and PMN–0.33PT, is of particular interest due to its higher Curie temperature compared to PMN–PT [9–11]. Detailed investigations of PT-based solid-solution phase diagrams have revealed the presence of an orthorhombic/monoclinic bridging phase in the MPB region, where the crystal structure changes abruptly [12–14]. Moreover, the monoclinic symmetry can coexist with a secondary minority rhombohedral or tetragonal phase [15]. Orthorhombic/monoclinic or mixed phases for PIN–PMN–PT crystals have been recently observed near the MPB [16,17]. The perovskite ferroelectrics possess a local, randomly oriented, nonreversible polarization below the Burns temperature T_d and exhibit deviations in the linearity of their refractive index $n(T)$ above T_d [18].

The temperature dependence of the band gap energy from interband transitions can provide important information about electron–phonon interactions and absorption characteristics [19,20]. Recently, we reported a negative band narrowing trend for rhombohedral PMN–0.24PT crystal and a positive trend for PMN–0.31PT crystal [21]. Motivated by the lack of studies on the temperature dependence of interband electronic transitions for tetragonal and MPB-related relaxor single-crystal ferroelectrics, we now try to answer questions concerning details of the abnormal temperature variation of the band structure. One can reasonably expect that the optical response behaviors could present some novel variations for relaxor ferroelectric crystals near the MPB, as compared to the ferroelectric and electrical properties. In this paper, we systematically investigate the transmittance spectra from rhombohedral, monoclinic and tetragonal PIN–PMN–PT crystals coexisting near the MPB. A model of the band structure is proposed to explain the composition dependence of the band gap near the MPB and the change in sign of the temperature variation trends with increasing PT content in the PMN–PT/PIN–PMN–PT system.

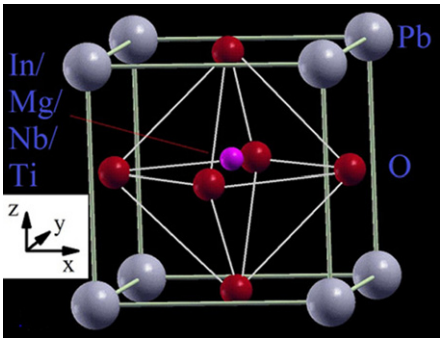

Fig. 1. The structure of perovskite PIN–PMN–PT.

2. Experimental details

PIN–PMN–PT single crystals were grown using a vertical Bridgman technique [22]. The samples were cut perpendicular to the ⟨001⟩ direction to give samples about 0.31 mm thick. The nominal composition of the xPIN–$(1-x-y)$PMN–yPT crystals obtained were $x \sim 0.27$–0.28 and $y \sim 0.29$–0.35. The PT content increases along the growth direction due to the segregation of Ti, resulting in a change in crystal structure and phase. The crystal structure of the PIN–PMN–PT crystals was analyzed by X-ray diffraction (XRD) using Cu $K\alpha$ radiation (D/MAX-2550 V, Rigaku Co.). The optical transmittance of the samples was recorded by a double-beam ultraviolet–infrared spectrophotometer (PerkinElmer UV/VIS Lambda 950) at photon energies of 0.5–6.5 eV (2650–190 nm) with an interval of 2 nm. The samples were mounted on a cold stage of an optical cryostat (Janis SHI-4-1) and the experimental temperature was controlled between 300 and 8 K by a temperature controller (Lakeshore 331).

3. Results and discussion

3.1. XRD analysis

It is clear from Fig. 2 that the XRD pattern changes with PT content. The position of the observed diffraction peaks increases with increasing PT content and the (200) diffraction splits into two peaks, i.e. the (002) and (200) profiles. As we know, the XRD profiles of the

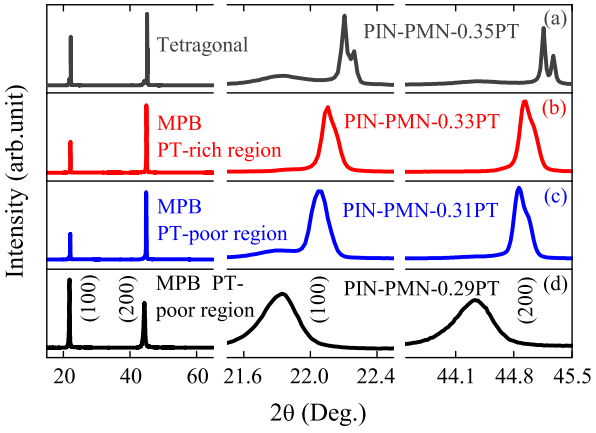

Fig. 2. The XRD patterns of the four PIN–PMN–PT crystals at room temperature.

(200) diffraction show only a single peak (200) in the rhombohedral phase due to this phase having the same lattice parameters for all the planes of (200), while the (200) diffraction peak is split in the tetragonal structure [6]. According to the reported phase diagram of PIN–PMN–PT/PMN–PT solid solutions and the diffraction patterns, the dominant phase of the PIN–PMN–0.35PT crystal is tetragonal and other PIN–PMN–PT crystals are in the MPB region [15–17]. Therefore, we divide the MPB region into a PT-rich region for PIN–PMN–0.33PT crystal and a PT-poor region for PIN–PMN–0.31PT and PIN–PMN–0.29PT crystals, based on the different thermodynamic stabilities of the phases, which will be discussed in the following.

3.2. Transmittance spectra

Fig. 3 and its insets show that the transmittance spectra of the PIN–PMN–PT crystals are nearly transparent from the visible to the near-infrared region and decrease with increasing photon energy, down to zero in the ultraviolet region. The largest variation of transmittance spectra with decreasing temperature is observed in the visible region, which is close to the onset of the electronic density of states (DOS) at the conduction band [23]. The conduction bands are considered to be mainly from Nb 4*d* near the band gap but come from Pb 6*p* above 5 eV based on a first-principles study of PMN [23]. The electronic DOS at the conduction band edge comes primarily from Nd *d* states in addition to Pb *p* and Mg/In *d* states, which indicates that Nd *d* states

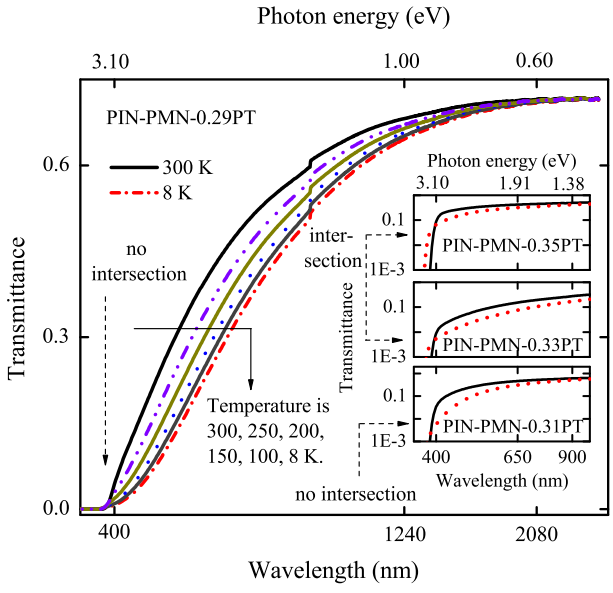

Fig. 3. Transmittance spectra of the PIN–PMN–0.29PT crystals at temperatures of 8, 100, 150, 200, 250, 300, respectively. (Inset) Transmittance spectra of the PIN–PMN–0.31PT, PIN–PMN–0.33PT and PIN–PMN–0.35PT crystals at the temperatures of 8 and 300 K, respectively. Horizontal direction is logarithmic coordinate for all four PIN–PMN–PT spectra and vertical direction of each spectrum in the inset is also logarithmic coordinate for clarity.

play a more important role than Mg/In *d* states in the conduction band. Noticeable Pb *p* character and Nb *d* character are found at the bottom of the O *p* bands, while no Mg/In *d* character is obvious in the valence bands. Although Pb *p*–O *p* hybridization is not the strongest interaction for the purpose of the O crystal field, Pb–O hybridization plays an important role in the polar characteristics.

An intersection point is observed near the absorption edge only for the PIN–PMN–0.35PT and PIN–PMN–0.33PT crystals in log coordinates. Interestingly, the absorption edges of the PIN–PMN–0.35PT and PIN–PMN–0.33PT crystals show a blueshift trend with decreasing temperature, while the trends of the other two compositions are opposite. The band gaps of most perovskite ferroelectric materials, e.g. $Bi_{3.25}La_{0.75}Ti_3O_{12}$ and $BiFeO_3$, were reported to increase with decreasing temperature [19,20]. As we know, the strain effect originating from thermal expansion affects the optical properties near the absorption edge mainly due to its influence on orbital overlap. The normal temperature dependence of the band gap in the PIN–PMN–0.35PT and PIN–PMN–0.33PT crystals can be explained by electron–phonon interaction and thermal expansion, the coefficients of which are about 3×10^{-6} K^{-1} near the MPB [24]. The rhombohedral PMN–0.2PT, the rhombohedral/monoclinic PMN–0.3PT, and the tetragonal PMN–0.35PT ceramics were reported to have the similar positive thermal expansion coefficients, from 2×10^{-6} K^{-1} to 3.2×10^{-6} K^{-1} [24]. However, the temperature dependence of interband electronic transitions in the multiphase PIN–PMN–0.31PT and PIN–PMN–0.29PT crystals are completely different from those of the PIN–PMN–0.35PT and PIN–PMN–0.33PT crystals, which indicates that other dominant factor must be considered to elucidate the abnormal optical properties in the MPB region.

3.3. A model of band structure to explain the positive and negative band narrowing trends

It is known that the phase of PT-based solid solutions varies with composition and temperature. A lower-symmetry phase(s) (monoclinic/orthorhombic) exists/coexists with either the rhombohedral phase or the tetragonal phase in the MPB region [12–15]. Apart from the well-known first-order tetragonal–cubic phase transition at high temperatures, a second characteristic anomaly related to the tetragonal/rhombohedral–monoclinic transition also exists at low temperatures. The coexistence of the tetragonal and monoclinic phases is observed below room temperature for PMN–0.38PT and PIN–0.4PT crystals [25,26]. The coexistence of multiphase stability changes with temperature. For the PIN–PMN–0.31PT and PIN–PMN–0.29PT crystals, rhombohedral domains coexist with monoclinic domains. As the temperature increases from 8 to 300 K, the rhombohedral domains increase rapidly at the expense of monoclinic domains. Similar hidden phase transformations are also observed in the PMN–PT crystals below room

temperature [27]. PIN–PMN–PT crystals are disordered and nonhomogeneous materials, whose highest structural disorder is found in the vicinity of the MPB. The phase transitions are the effect of the correlated ion off-center displacement. In the PT-rich region of the MPB, the coexistence of the rhombohedral and monoclinic phases of the PIN–PMN–0.33PT crystal is thermodynamically stable while in the PT-poor region of the MPB, the rhombohedral phase becomes metastable for the PIN–PMN–0.31PT and PIN–PMN–0.29PT crystals due to the stress-relaxation effect. The phenomenon that similar transformation stress induces a metastable phase has recently been reported for $Pb(Zn_{1/3}Nb_{2/3})_3$–$PbTiO_3$ crystals in the PT-poor region of the MPB [28].

3.3.1. Calculation for rhombohedral or tetragonal single-phase region

The band gap energy E_g of most semiconductors and PMN–PT/PIN–PMN–PT solid-solution systems with a single phase (except the multiphase MPB region) decreases with increasing temperature T, according to:

$$E_g(T) > E_g(T+\Delta T), \tag{1}$$

where $8\ \mathrm{K} < T < T+\Delta T < 300\ \mathrm{K}$ in the present experiment. Fig. 4a shows that the $E_g(T)$ of rhombohedral PMN–0.24PT [21] and tetragonal PIN–PMN–0.35PT decrease with T. From Eq. (1) and $E_g = E_c - E_d$, where E_c is the bottom of the conduction band and E_v is the top of the valence band, we deduce:

$$\begin{aligned} E_c(T) - E_v(T) &= E_g(T) > E_g(T+\Delta T) \\ &= E_c(T+\Delta T) - E_v(T+\Delta T). \end{aligned} \tag{2}$$

Obviously, $E_g(T)$ is dependent on the difference between $E_c(T)$ and $E_v(T)$ rather than the absolute location of $E_c(T)$ or $E_v(T)$. Therefore, we indicate a lowering of the conduction-band states with increasing temperature while the valence-band states of different phases and different temperature remain stationary to make the schematic representation in Figs. 4 and 5 simple. The band narrowing variation $\Delta E_g = E_g(T+\Delta T) - E_g(T)$ is negative in the rhombohedral or tetragonal phase regions.

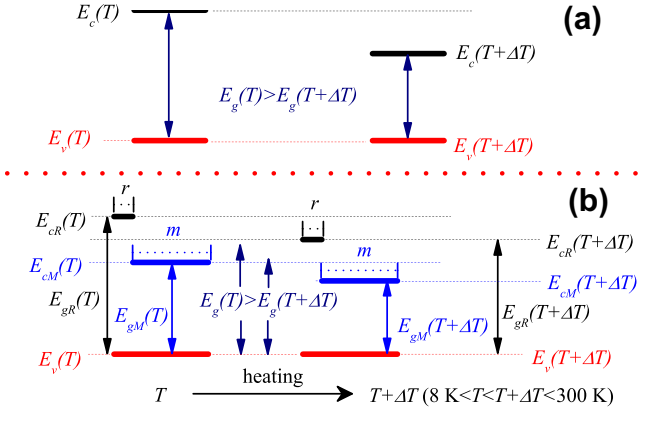

Fig. 4. (a) Schematic representation of the valence and conduction bands at temperature T and $T+\Delta T$ for rhombohedral PMN–0.24PT [21], tetragonal PIN–PMN–0.35PT and (b) PIN–PMN–0.33PT crystals in the PT-rich region of the MPB where the rhombohedral and monoclinic phases coexist stably.

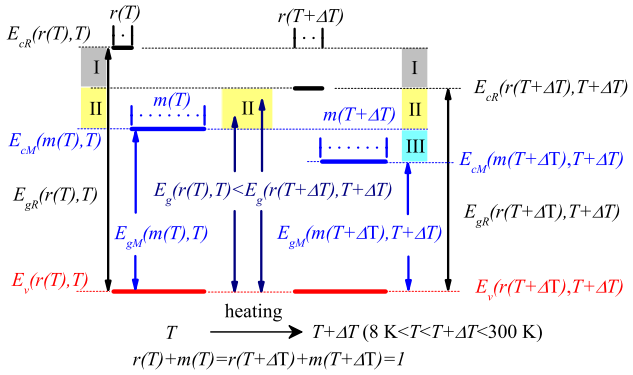

Fig. 5. Schematic representation of the valence and conduction bands at temperature T and $T+\Delta T$ for PMN–0.31PT [21], PIN–PMN–0.31PT and PIN–PMN–0.29PT crystals in the PT-poor region of the MPB where the rhombohedral and monoclinic phases coexist unstably.

3.3.2. Calculation for PT-rich region of the MPB: stationary multiphase coexistence

The band gap energy E_g decreases with increasing PT content x in PMN–xPT and PZN–xPT at room temperature [21,29,30], according to:

$$E_g(x) > E_g(x+\Delta x), \quad 0 \leqslant x < x+\Delta x \leqslant 1 \tag{3}$$

From Eqs. (1) and (3), we conclude that $E_g(x,T)$ is a function of the PT content x and temperature T. Furthermore, R phase changes into R + M phases coexisting, and then into T phase with increasing PT content x, where R, M and T are the rhombohedral, monoclinic and tetragonal phases, respectively. The expression below is deduced from Eq. (3):

$$E_{gR} > E_{gM} > E_{gT}, \tag{4}$$

where E_{gR},E_{gM} and E_{gM} are the band gap energy E_g for the R, T and M phases, respectively. Therefore, $E_g(r,T)$ is a function of the R phase content r and temperature T in the R + M phase region, where the relation between the M phase content m and R phase content r is:

$$m = 1 - r, \quad 0 < r < 1, \quad 0 < m < 1. \tag{5}$$

The expression for $E_g(r,T)$ in the stationary R + M phase region is:

$$\begin{aligned} E_g(r,T) &= E_g(r = constant, T) = E_g(T) \\ &= k_r r E_{gR}(T) + k_m m E_{gM}(T) \\ &= k_r r E_{gR}(T) + k_m (1-r) E_{gM}(T), \\ & \quad k_r > 0, \ \ k_m > 0 \end{aligned} \tag{6}$$

where k_r and k_m are the respective contribution coefficients of the R phase and M phase to the band gap energy E_g. Obviously, $k_r = 1$, $r = 1$ and $E_g = E_{gR}$ when the PMN–PT/PIN–PMN–PT is in the rhombohedral phase region. The contribution coefficient and band gap energy have a

similar relation in the tetragonal phase region. With increasing temperature, $E_g(r,T)$ becomes $E_g(r,T+\Delta T)$, having the following form:

$$E_g(r,T+\Delta T) = E_g(T+\Delta T) = k_r r E_{gR}(T+\Delta T) + k_m(1-r)E_{gM}(T+\Delta T). \quad (7)$$

From Eq. (1), we deduce:

$$E_{gR}(T) > E_{gR}(T+\Delta T), \quad E_{gM}(T) > E_{gM}(T+\Delta T). \quad (8)$$

Therefore, Eq. (6) > Eq. (7), and the band narrowing variation ΔE_g is negative in the stationary R + M phase region.

3.3.3. Calculation for the PT-poor region of the MPB: intense multiphase competition

In the region in which the R + M phases exist in competition, the R phase content r is a function of temperature T, $r(T)$, rather than a constant. Eq. (5) then changes into the form:

$$m(T) = 1 - r(T), \quad 0 < r(T) < 1, \quad 0 < m(T) < 1. \quad (9)$$

Eq. (6) in the present region is:

$$E_g(r(T),T) = k_r r(T)E_{gR}(T) + k_m m(T)E_{gM}(T) = k_r r(T)E_{gR}(T) + k_m(1-r(T))E_{gM}(T), \quad (10)$$

where $E_{gM}(r(T),T) < E_g(r(T),T) < E_{gR}(r(T),T)$. $E_g(r(T),T)$ is located in regions I–II, as shown in Fig. 5.

When T becomes $T+\Delta T$, Eq. (10) changes into the form:

$$E_g(r(T+\Delta T),T+\Delta T) = k_r r(T+\Delta T)E_{gR}(T+\Delta T) + k_m(1-r(T+\Delta T))E_{gM}(T+\Delta T), \quad (11)$$

where $E_{gM}(r(T+\Delta T),T+\Delta T) < E_g(r(T+\Delta T),T+\Delta T) < E_{gR}(r(T+\Delta T),T+\Delta T)$. $E_g(r(T+\Delta T),T+\Delta T)$ is located in regions II–III, as shown in Fig. 5. Comparing the first term in Eqs. (10) and (11),

$$r(T) < r(T+\Delta T), \quad E_{gR}(T) > E_{gR}(T+\Delta T), \quad (12)$$

the numerical comparison between $r(T)E_{gR}(T)$ and $r(T+\Delta T)E_{gR}(T+\Delta T)$ becomes complicated.

Differentiation is a method to compute the rate where a dependent output $E_g(r(T),T)$ changes with respect to the change in the independent input T. Finding a derivative of $E_g(r(T),T)$, we obtain:

$$E_g'(r(T),T) = \frac{\partial E_g(r(T),T)}{\partial r}\frac{dr}{dT} + \frac{\partial E_g(r(T),T)}{\partial T}. \quad (13)$$

The first term in Eq. (13) is the contribution of the variation of R phase content r to the band gap energy E_g; the second term is the thermal motion. The first term in Eq. (13) is positive due to the R phase content r increment at elevated temperatures, while the second term is negative according to Eq. (1). The temperature dependence of the energy band gap in the PT-poor region of the MPB is positive because the variation of R phase content r $\left(\frac{\partial E_g(r(T),T)}{\partial r}\frac{dr}{dT}\right)$ is more sensitive than the thermal effect $\left(\frac{\partial E_g(r(T),T)}{\partial T}\right)$. The situation is shown in Fig. 5. The band narrowing variation ΔE_g is positive in the region in which multiple phases are in competition.

3.4. Direct and indirect transitions

The electronic interband transitions of the PIN–PMN–PT crystals include both direct and indirect processes. Similar phenomena have been found in ferroelectric PZN–PT, PMN–PT and $Bi_4Ti_3O_{12}$ by both experiments and calculations [21,30–32]. In the direct transition an electron jumps from the band at lower energy to the one above it by absorbing a photon, while in the indirect transition both photons and phonons are necessary to satisfy conservation of energy and crystal momentum. Indirect transition is a second-order process, which means that a photon must be destroyed and a phonon must be either created or destroyed. In contrast, direct transition is a first-order process because no phonons are involved. In the direct transition, the absorption coefficient α as a function of photon energy is expressed by the Tauc relation [33]: $\alpha h\upsilon \propto (h\upsilon - E_{gd})^{1/2}$, where υ is the frequency, h is Planck's constant and E_{gd} is the allowed direct band gap. In the indirect transition, the absorption coefficient is expressed as $\alpha h\upsilon \propto (h\upsilon - E_{gi} \mp E_p)^2$, where E_{gi} is the indirect band gap and E_p is the energy of the absorbed (+) or emitted (−) phonon. The values of E_{gd}, $E_{g1} = E_{gi} + E_p$ and $E_{g2} = E_{gi} - E_p$ can be obtained by extrapolating the linear portion of the respective curves to zero. The schematic band structure of PMN-PT/PIN-PMN-PT is shown in Fig. 6a. The

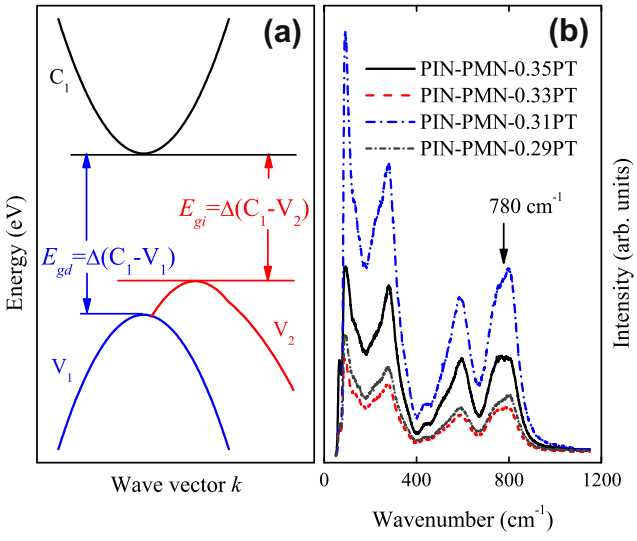

Fig. 6. (a) Schematic band structure of PMN-PT/PIN-PMN-PT. (b) Raman spectra of PIN–PMN–0.35PT, PIN–PMN–0.33PT, PIN–PMN–0.31PT and PIN–PMN–0.29PT crystals at room temperature.

phonon energy calculated from the transmittance spectra is 0.1 eV (806 cm^{-1}), which agrees with the 780 cm^{-1} mode recorded by Raman spectroscopy in Fig. 6b. The 780 cm^{-1} phonon mode, corresponding to Nb–O–Mg/In stretching vibrations in analogy with the Nb–O–Mg mode in PMN, assists the transition. The phonon mode at 780 cm^{-1} is sensitive to the distortion of the BO_6 octahedra, exhibiting obvious temperature and polarization dependence. The mode intensity attenuates in $\langle x|zx|y\rangle$ (VH) geometry with increasing temperature, while it does not show significant temperature variations in the parallel $\langle x|zz|y\rangle$ (VV) geometry, demonstrating a A_{1g} phonon mode character [34,35]. Moreover, the lattice vibration is sensitive to the PT content due to the change in crystal symmetry.

The PIN–PMN–PT crystals have an absorption edge in the ultraviolet spectral region, caused by the onset of optical transitions across the fundamental band gap. The values of the direct band gap E_{gd} and indirect band gap E_{gi} are evaluated, and the temperature variations are shown in Fig. 7a and b, respectively. The direct band gap of the PIN–PMN–0.35PT and PIN–PMN–0.33PT crystals decreases with increasing temperature due to the normal thermal effect, while for the PIN–PMN–0.31PT and PIN–PMN–0.29PT crystals the situation is reversed, which is mainly due to B-site cation disorder and oxygen octahedral tilts leading to instability of multiphase coexistence at low temperature. The temperature dependence of the E_{gd} is given by [19,20]:

$$E_{gd}(T) = E_{gd}(T = 0\ \mathrm{K}) - 2a_B/[\exp(\Theta_B/T) - 1] \quad (14)$$

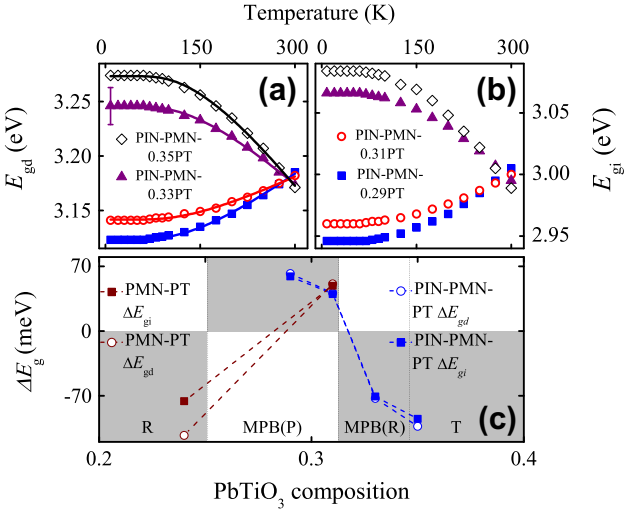

Fig. 7. Temperature dependence of (a) the direct band gaps and (b) the indirect band gaps of the PIN–PMN–PT crystals. The fitting results using Eq. (14) are plotted with a solid line. A representative error bar is shown. (c) The direct and indirect band gap narrowing variation as a function of PT content for the PMN–PT/PIN–PMN–PT crystals near the MPB. The signals R, MPB (P), MPB (R) and T represent the rhombohedral phase region, the PT-poor region in the morphotropic phase boundary, the PT-rich region in the morphotropic phase boundary, and the tetragonal phase region, respectively. Light gray rectangles are the regions of band gap narrowing variation.

Table 1
The parameter values of Eq. (14) and band narrowing coefficient dE_{gd}/dT.

PT content	$E_{gd}(T = 0\ \mathrm{K})$ (eV)	a_B (meV)	Θ_B (K)	dE_{gd}/dT (300 K) ($\times 10^{-4}$ eV/K)
0.29	3.12	**−108**	458	3.90
0.31	3.14	**−68**	448	2.54
0.33	3.25	134	468	−4.69
0.35	3.27	205	486	−6.79

where a_B is the coupling interaction strength, and Θ_B is the average phonon temperature. The fitted parameter values and band narrowing coefficient dE_{gd}/dT are summarized in Table 1, and the fitting E_{gd} curves are shown in Fig. 7a by solid lines. The coupling interaction strength a_B and E_{gd} increases with PT content x: $a_B(x) = (-1.79 \pm 0.34)x + (5.71 \pm 1.07)$ eV, $E_{gd}(T = 0\ \mathrm{K})(x) = (2.77 \pm 0.58)x + (2.31 \pm 0.19)$ eV. However, the irregular variation of Θ_B with PT content x makes the expression somewhat complex: $\Theta_B(x) = 0.218 - 1.967x + 6x^2 - 6.062x^3$ 10^5 K, $(0.29 \leqslant x \leqslant 0.33)$.

The direct and indirect band gap narrowing variation ΔE_g close to the MPB in the schematic phase diagram for the present PIN–PMN–PT and the previous PMN–PT crystals are shown in Fig. 7c. This phase diagram can be roughly divided into four regions: a rhombohedral phase (e.g. PMN–0.24PT crystal) [21]; a PT-poor region in the MPB where multiphase competition occurs with increasing temperature (e.g. PMN–0.31PT [21], PIN-PMN-0.29PT and PIN–PMN–0.31PT crystals); a PT-rich region in the MPB where a stationary multiphase exists (e.g. PIN–PMN–0.33PT crystal); and a tetragonal phase (e.g. PIN–PMN–0.35PT crystal). The positive ΔE_g is only found in the PT-poor region of the MPB, while it becomes negative in the rhombohedral, tetragonal and the PT-rich regions of the MPB. The positive band gap narrowing variation in the PT-poor region near the MPB is due to a long-range increasing fraction of coexistence from the monoclinic to rhombohedral transition with increasing temperature.

3.5. Origin of the phase transition

What is the origin of the hidden transition? It is the competition between oxygen octahedra tilting and phonon entropy that determines the MPB [36]. The Gibbs free energy is defined as: $G(P, T) = U + PV - TS$, where U is the internal energy, P is pressure, V is volume, T is the temperature and S is the entropy. The entropy term TS prefers the rhombohedral structure, dominating at elevated temperatures, while the term PV favors oxygen octahedra tilting of the monoclinic phase, dominating at the lowest temperature. The phonon contribution does not prefer one phase to the other at the lowest temperature because the low-frequency parts of the phonon DOS for the different phases are similar [37,38]. Moreover, a crystal lattice lies in its ground state, containing no phonon at absolute zero temperature. Random lattice vibrations lead to energy

fluctuations of the lattice at a non-zero temperature, resulting a deviation of atoms or ions from equilibrium sites and a perturbation of electron energy and transition. The phonon contribution to the Helmholtz free energy, which consists of contributions to the internal energy and entropy, is smaller than the difference between the rhombohedral and monoclinic phases at low temperature. The lattice vibration is enhanced with increasing temperature, reinforcing the electron–phonon interaction and resulting in a thermally modified band structure. On the other hand, the strain originating from thermal energy can induce antiferrodistortive displacement, corresponding to the tilting of the oxygen octahedra simultaneously with the ferroelectric cation displacements [15]. The octahedra tilting is seen in the case of the monoclinic phase because it gives rise to changes in bond lengths and angles accompanied by an efficient volume compression. Both mechanisms were reported to coexist even above room temperature at high pressures in ferroelectric perovskite lead zirconate titanate [$Pb(Zr_xTi_{1-x}O_3)$] in the vicinity of the MPB [36].

4. Summary

To summarize, we have investigated the temperature-dependent transmittance spectra of ferroelectric PIN–PMN–PT crystals around the MPB. The band narrowing coefficients dE_{gd}/dT for PIN–PMN–PT crystals in the vicinity of the MPB are found to be different, depending on the distinct crystal structures and phases. The coexistence and competition of multiple phases of the PIN–PMN–PT crystals, and how they affect the band gap shrinkage with temperature, are discussed. The proposed multiphase model of the band structure can explain the positive and negative temperature coefficient of the band gap around the MPB. The present model suggests that a positive coefficient may exist when two criteria are met: (i) the coexistence of two or more phases; and (ii) the multiphase structure is unstable with temperature.

Acknowledgments

J.J.Z. thanks H.C. Ding for technical support. This work was supported by NSFC (Grant Nos. 60906046 and 11074076), Major State Basic Research Development Program of China (Grant Nos. 2007CB924901, and 2011CB922200), Program of NCET, MOE (Grant No. NCET-08-0192) and PCSIRT, Science and Technology Commission of Shanghai Municipality Project (Grant Nos. 10DJ1400201, 10SG28, 10ZR1409800 and 09ZZ42), the High Technology and Development Project of China (Grant No. 2008AA03Z411) and the Program for Professor of Special Appointment (Eastern Scholar) at Shanghai Institutions of Higher Learning.

References

[1] Fan HY. Phys Rev 1951;82:900.
[2] Dimmock JO, Melngailis I, Strauss AJ. Phys Rev Lett 1966;16:1193.
[3] Tsang YW, Cohen ML. Phys Rev B 1971;3:1254.
[4] Chadi DJ, Cohen ML. Phys Rev B 1973;7:692.
[5] Park SE, Shrout TR. J Appl Phys 1997;82:1804.
[6] He C, Li XZ, Wang ZJ, Long XF, Mao SY, Ye ZG. Chem Mater 2010;22:5588.
[7] Noheda B, Cox DE, Shirane G, Park SE, Cross LE, Zhong Z. Phys Rev Lett 2001;86:3891.
[8] Fu H, Cohen RE. Nature (London) 2000;403:281.
[9] Zhang SJ, Luo J, Li F, Meyer Jr RJ, Hackenberger W, Shrout TR. Acta Mater 2010;58:3773.
[10] Lin DB, Lee HJ, Zhang SJ, Li F, Li ZR, Xu Z, et al. Scripta Mater 2011;64:1149.
[11] Webber KG, Robinson HC, Rossetti Jr GA, Lynch CS. Acta Mater 2008;56:2744.
[12] Xu GS, Luo HS, Xu HQ, Yin ZW. Phys Rev B 2001;64:020102. R.
[13] La-Orauttapong D, Noheda B, Ye ZG, Gehring PM, Toulouse J, Cox DE, et al. Phys Rev B 2001;65:144101.
[14] Long XF, Ye ZG. Acta Mater 2007;55:6507.
[15] Noheda B, Cox DE. Phase Transit 2006;79:5.
[16] Li F, Zhang SJ, Xu Z, Wei XY, Luo J, Shrout TR. Appl Phys Lett 2010;97:252903.
[17] Sun EW, Zhang SJ, Luo J, Shrout TR, Cao WW. Appl Phys Lett 2010;97:032902.
[18] Burns G, Dacol FH. Phys Rev B 1983;28:2527.
[19] Hu ZG, Li YW, Yue FY, Zhu ZQ, Chu JH. Appl Phys Lett 2007;91:221903.
[20] Li WW, Zhu JJ, Wu JD, Gan J, Hu ZG, Zhu M, et al. Appl Phys Lett 2010;97:121102.
[21] Zhu JJ, Li WW, Xu GS, Jiang K, Hu ZG, Zhu M, et al. Appl Phys Lett 2011;98:091913.
[22] Xu GS, Chen K, Yang DF, Li JB. Appl Phys Lett 2007;90:032901.
[23] Suewattana M, Singh DJ. Phys Rev B 2006;73:224105.
[24] Wongmaneerung R, Guo RY, Bhalla A, Yimnirun R, Anata S. J Alloys Compd 2008;461:565.
[25] Slodczyk A, Daniel P, Kania A. Phys Rev B 2008;77:184114.
[26] Tu CS, Wang FT, Hung CM, Chien RR, Luo HS. J Appl Phys 2006;100:104104.
[27] Chien RR, Schmidt VH, Hung LW, Tu CS. J Appl Phys 2005;97:114112.
[28] Chang WS, Lim LC, Yang P, Ku CS, Lee HY, Tu CS. J Appl Phys 2010;108:044105.
[29] Chan KY, Tang WS, Mak CL, Wong KH. Phys Rev B 2004;69:144111.
[30] Sun EW, Zhang R, Wang Z, Xu DP, Li L, Cao WW. J Appl Phys 2010;107:113532.
[31] Singh DJ, Seo SSA, Lee HN. Phys Rev B 2010;82:180103. R.
[32] Shimakawa Y, Kubo Y, Tauchi Y, Asano H, Kamiyama T, Izumi F, et al. Appl Phys Lett 2001;79:2791.
[33] Tauc JC. Optical Properties of Solids. Amsterdam: North-Holland; 1972.
[34] Svitelskiy O, Toulouse J, Yong G, Ye ZG. Phys Rev B 2003;68:104107.
[35] Kamba S, Buixaderas E, Petzelt J, Fousek J, Nosek J, Bridenbaugh P. J Appl Phys 2003;93:933.
[36] Frantti J, Fujioka Y, Zhang J, Vogel SC, Wang Y, Zhao Y, et al. J Phys Chem B 2009;113:7967.
[37] Prosandeev SA, Cockayne E, Burton BP, Kamba S, Petzelt J, Yuzyuk Y, et al. Phys Rev B 2004;70:134110.
[38] Choudhury N, Wu ZG, Walter EJ, Cohen RE. Phys Rev B 2005;71:125134.